NATIONAL ADVISORY COMMITTEE FOR AERONAUTICS

WARTIME REPORT

ORIGINALLY ISSUED

October 1942 as
[redacted]Report

AN INVESTIGATION OF AIRCRAFT HEATERS

III - MEASURED AND PREDICTED PERFORMANCE OF DOUBLE TUBE HEAT EXCHANGERS

By R. C. Martinelli, E. B. Weinberg
E. H. Morrin, and L. M. K. Boelter
University of California

NACA

WASHINGTON

NATIONAL ADVISORY COMMITTEE FOR AERONAUTICS

[redacted] REPORT

AN INVESTIGATION OF AIRCRAFT HEATERS

III - MEASURED AND PREDICTED PERFORMANCE

OF DOUBLE TUBE HEAT EXCHANGERS

By R. C. Martinelli, E. B. Weinberg,

E. H. Morrin, and L. M. K. Boelter

INTRODUCTION

Two double tube cylindrical heat exchangers, in which hot exhaust gases pass through the annular space and ventilating air passes through the center tube, have been tested to determine heat transfer performance and pressure drop. One of the exchangers was equipped with a smooth cylindrical air pipe (fig. 4), while the other utilized a dimpled type intensifier tube (fig. 5).

The tests were performed in order

1. To establish a simple, accurate method of predicting the performance of the double tube heat exchanger, since this design is a basic element of practically all gas-air heaters.

2. To compare the performance of the straight and dimpled tubes.

3. To determine the pressure drop across the units.

EXPERIMENTAL EQUIPMENT

In brief, the experimental equipment consisted of a source of hot gases and a source of cool air. These were metered and passed through the heater being tested.

Measurement of appropriate temperatures and pressures allowed the calculation of the performance of the heater. Two sources of hot gases were utilized. The exhaust gases from a 50-horsepower gasoline engine were used at first, but it was discovered that hot gases from a natural gas burner yielded essentially the same results with much less operational difficulty. The latter method is utilized at present.

Gasoline Engine Test Stand*

An analysis of the thermal resistances existing in the double tube heat exchanger (see p. 7) indicated that the fundamental parameters governing the rate of heat transfer were the gas temperature and the weight rate of gas flow per unit area. The latter parameter may be varied by changing either the weight rate of gas flow or the cross-sectional area through which the gas moves.

In absence of a large engine capable of producing high exhaust gas rates, a small (50 hp) engine was utilized to produce the hot gases, and high weight rates per unit area were obtained by the use of a small exhaust gas annulus (O.D. = 3.07 in., I.D. = 2.00 in.).

The ventilating air was supplied to the heaters by a Roots-type blower of 1000 cubic feet per minute capacity.

The flow of exhaust gases was obtained by metering the fuel and combustion air to the engine. It was not necessary to meter the hot exhaust gases, since the weight rate per unit cross-sectional area is the important parameter which can be obtained by metering the fuel and combustion air to the engine. The latter measurements were more easily obtained. The flow of ventilating air was measured by means of a calibrated $1\frac{1}{4}$-inch sharp-edge orifice.

Temperatures were obtained at the following points:

1. Ventilating air into heat exchanger

2. Ventilating air out of heat exchanger (see p. 18)

3. Exhaust gases into heat exchanger

4. Exhaust gases out of heat exchanger

5. Ventilating air tube wall (4 points)

6. Outer tube of exhaust gas annulus (4 points)

The exhaust gas temperatures were obtained by means of the shielded thermocouples proposed by the American Society of Mechanical Engineers (reference 1). Chromel-alumel thermocouples were used throughout.

Pressure drop along the ventilating air tube and the annular exhaust space were measured by means of U-tube water manometers. Carefully installed piezometer rings were used on the air tube, but, owing to the construction of the gas annulus, single pressure tap holes were of necessity utilized on the exhaust gas stream.

Engine speed, load, exhaust gas analysis, barometric pressure, and air humidity were also determined. The entire heater unit was surrounded by 2 inches of sand.

A schematic diagram of the gasoline engine test stand is shown in figure 1.

Natural Gas Test Stand

The natural gas test stand (fig. 2) utilized a 1,000,000 Btu per hour gas burner to create the hot gases. The flame from the burner was conducted through a converging section to the exhaust gas annulus. Part of the secondary air was supplied by a small blower in order to insure complete combustion before the gases struck the ventilating air tube.

The gas flow was controlled by means of a centrifugal exhaust fan located downstream from the heat exchanger.

The rate of exhaust gas flow was measured by means of a calibrated $1\frac{1}{2}$- by 3-inch venturi meter placed between the heater and the exhaust fan.

All other measurements were made in the same manner as with the gasoline engine test stand.

SYMBOLS

A_a heat-transfer area of air side, ft^2

A_g heat-transfer area of gas side, ft^2

A_w surface area of outer tube of annulus, ft^2

c_p unit heat capacity of air at constant pressure, Btu/lb °F

C constant

D diameter, ft

D_a inner diameter of air tube, ft

D_g hydraulic diameter of gas annulus, ft

e_1, e_2 emissivities of inner and outer surfaces of annulus, respectively

f_c unit thermal convective conductance, Btu/hr ft^2 $^\circ$F

f_{ca} unit thermal convective conductance on air side, Btu/hr ft^2 $^\circ$F

f_{cg} unit thermal convective conductance on gas side, Btu/hr ft^2 $^\circ$F

f_r equivalent unit thermal conductance for radiation, Btu/hr ft^2 $^\circ$F

F_A shape modulus, the factor in the radiation equation which allows for the geometrical position of the radiating surfaces

F_E emissivity modulus, the factor in the radiation equation which allows for the non-Planckian character of the radiation surfaces

g gravitational force per unit mass, lb/(lb sec^2/ft)

G weight rate of flow per unit area, lb/hr ft^2

G_a weight rate of flow per unit area for air, lb/hr ft^2

G_g weight rate of flow per unit area for gas, lb/hr ft^2

k_a thermal conductivity of air, Btu/hr ft^2 ($^\circ$F/ft)

N distance between pressure taps, ft

P pressure, lb/ft^2

P_1 pressure at entrance to heat exchanger, lb/ft^2

P_2 pressure at exit from heat exchanger, lb/ft^2

q_a predicted rate of heat transfer, Btu/hr

q_c rate of heat transfer by convection, Btu/hr

q_M measured rate of heat transfer, Btu/hr

q_r rate of heat transfer by radiation, Btu/hr

r radial coordinate measured from center line of tube, ft

r_o radius of pipe, ft

t_p average intensifier tube wall temperature, ^oF

t_w average temperature of outer wall of annulus, ^oF

T absolute temperature, ^oR

T_{a1}, T_1 mixed mean absolute temperature of air entering heating section, ^oR

T_{a2}, T_2 mixed mean absolute temperature of air leaving heating section, ^oR

T_a arithmetic average absolute temperature of air in heater, ^oR

T_g arithmetic average absolute temperature of gas in heater, ^oR

T_p average absolute temperature of intensifier tube wall, ^oR

T_w average absolute temperature of outer wall of annulus, ^oR

u velocity of fluid at any point r, ft/sec

u_{max} velocity of fluid at center of pipe, ft/sec

v mean velocity of fluid based on rate of discharge and pipe area, ft/sec

v_1 mean velocity of fluid at entrance to heating section, ft/sec

v_2 mean velocity of fluid leaving heating section, ft/sec

W_a air weight rate, lb/hr

W_g exhaust gas weight rate, lb/hr

x coordinate measured along tube, ft

y coordinate measured perpendicular to tube wall, ft

γ weight density of air at any temperature and pressure, lb/ft^3.

γ_1 weight density of air at entrance to heating section, lb/ft^3

γ_2 weight density of air leaving heating section, lb/ft^3

γ_T weight density of air at temperature T, lb/ft^3

ΔP pressure drop across pipe, lb/ft^2

ΔP_{T_1} isothermal pressure drop due to friction at temperature T_1, lb/ft^2

$\frac{\Delta P}{\Delta L}$ pressure drop per foot, $(lb/ft^2)/ft$

Δt difference in temperature between the tube wall and any point y in the fluid stream, $^{\circ}F$

$\Delta t_1 = (\tau_{g1} - \tau_{a1})$, $^{\circ}F$

$\Delta t_2 = (\tau_{g2} - \tau_{a2})$, $^{\circ}F$

Δt_{max} tube temperature minus temperature of fluid at center of stream, $^{\circ}F$

Δt_{mean} tube temperature minus temperature of fluid after complete mixing, $^{\circ}F$

Δt_{lm} logarithmic mean temperature difference, $^{\circ}F$

ζ isothermal friction factor

ζ_{T_1} isothermal friction factor for air at temperature T_1

ζ_{T_a} isothermal friction factor for air at temperature T_a

ζ_T isothermal friction factor for air at temperature T

μ viscosity of air, $lb\ sec/ft^2$

μ_T viscosity of air at temperature T, $lb\ sec/ft^2$

τ_{a1} mixed-mean temperature of air at entrance to heating section, $^{\circ}F$

τ_{a2} mixed-mean temperature of air leaving heating section, $^{\circ}F$

τ_{g1} mixed-mean temperature of gas at entrance to heating section, °F

τ_{g2} mixed-mean temperature of gas leaving heating section, °F

$$\tau_a = \frac{\tau_{a1} + \tau_{a2}}{2}, \ ^{\circ}F$$

$$\tau_g = \frac{\tau_{g1} + \tau_{g2}}{2}, \ ^{\circ}F$$

$$Nu = \frac{f_c D}{k}, \text{ Nusselt modulus}$$

$$Pr = \frac{\mu\ cp\ g\ 3600}{k}, \text{ Prandtl modulus}$$

$$Re = \frac{G D}{3600\ \mu\ g}, \text{ Reynolds modulus}$$

ANALYSIS OF MECHANISM OF HEAT TRANSFER IN DOUBLE TUBE HEAT EXCHANGERS

In a double tube heat exchanger, in which the exhaust gas flows in the annular space and the ventilating air in the central tube (fig. 3), the mechanism of heat transfer at any point along the length of the inner pipe proceeds as follows:

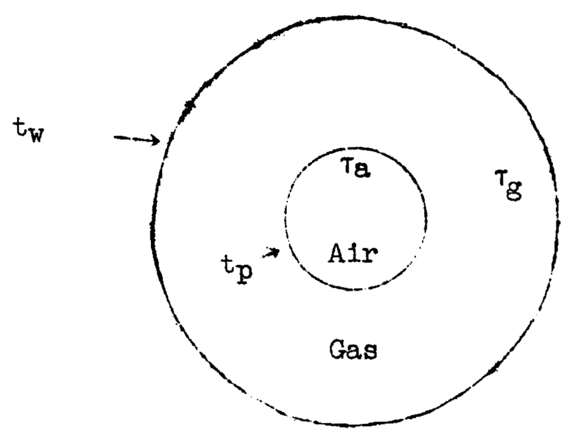

Figure 3.- Cross section of double tube heat exchanger.

(a) Heat flows from the exhaust gas to the inner tube by convection. The rate of convective transfer is given by:

$$dq_c = f_{cg}(\tau_g - t_p)dA_g \tag{1}$$

(b) Heat flows between the outer and the inner tube by radiation through a diathermanous* medium,

$$dq_r = 0.173\ F_A\ F_E \left[\left(\frac{T_w}{100}\right)^4 - \left(\frac{T_p}{100}\right)^4 \right] dA_g \tag{2}$$

For the tubular heat exchanger (reference 2, p. 54)

$$F_A = 1.00$$

$$F_E = \frac{1}{\frac{1}{e_1} + \frac{A_g}{A_w}\left(\frac{1}{e_2} - 1\right)} \tag{3}$$

An equivalent unit conductance for radiation may be defined so that

$$dq_r = f_r(\tau_g - t_p)dA_g \tag{4}$$

Thus,

$$f_r = \frac{0.173\ F_A\ F_E \left[\left(\frac{T_w}{100}\right)^4 - \left(\frac{T_p}{100}\right)^4 \right]}{(\tau_g - t_p)} \tag{5}$$

(c) Heat may be transferred to the inner tube by gaseous radiation from the H_2O and CO_2 present in the exhaust gas (reference 3, p. 297). A calculation reveals this quantity to be negligible in most cases.

(d) All of the heat which is transferred to the outer surface of the inner tube (the sum of the quantities discussed above) must be transferred to the air flowing through the inner tube by convection. Thus, if the gaseous radiation is neglected

---

*Affording a free passage to radiant energy.

$$dq_a = dq_c + dq_r = f_{ca}(t_p - \tau_a)dA_a \qquad (6)$$

The three equations (1), (4), (6) allow the prediction of the thermal performance of the heater. For simplicity, however, it is customary to eliminate the tube wall temperature from the equations (reference 4, p. XIV-1). Then, upon integration along the tube length*

$$q_a = \frac{\Delta t_{lm}}{\left[\frac{1}{(f_r + f_{cg})A_g} + \frac{1}{f_{ca}\,A_a}\right]} \qquad (7)$$

In equation (7)

(a) The logarithmic mean temperature difference may be determined readily from the measured magnitudes of the gas and air temperatures entering and leaving the exchanger. Thus:

$$\Delta t_{lm} = \frac{(\tau_{g1} - \tau_{a1}) - (\tau_{g2} - \tau_{a2})}{ln\left(\frac{\tau_{g1} - \tau_{a1}}{\tau_{g2} - \tau_{a2}}\right)} \qquad (8)$$

(b) The areas A_g and A_a are readily determined by measurement.

(c) The radiant unit conductance may be calculated by means of equation (5).

The magnitudes of the unit convective conductances f_{ca}, f_{cg} must now be predicted.

For the turbulent flow inside a circular tube, by reasoning based on an idealized analogy between heat and momentum transfer, it may be shown (reference 5, p. 447) that:

---

*The use of the log mean temperature difference Δt_{lm} is based on the postulate that $(f_r + f_{cg})$ and f_{ca} are independent of the tube length (as well as several other restrictions). (See reference 4, p. XIV-1.) Although all these postulates are not exactly satisfied by the experimental equipment, the utilization of the log mean temperature difference will be found to be sufficiently accurate.

$$\frac{Nu}{Re\ Pr} = \frac{f_c}{G\ c_p} = \frac{\sqrt{\frac{\zeta}{8}}\ \frac{\Delta t_{max}}{\Delta t_{mean}}}{5.0\left[Pr + \ln(1 + 5\ Pr) + 0.50\ \ln\left(\frac{Re}{60}\sqrt{\frac{\zeta}{8}}\right)\right]} \qquad (9)$$

where

ζ friction factor for smooth tubes defined by

$$\frac{\Delta P}{\gamma} = \zeta \frac{L}{D} \frac{v^2}{2g}$$

Δt_{max} tube temperature - temperature of fluid at center of stream, °F

Δt_{mean} tube temperature - temperature of fluid after complete mixing, °F

Pr Prandtl modulus

Re Reynolds modulus

Nu Nusselt modulus

A close empirical approximation of the more exact equation (9) was presented by Colburn (reference 6, p. 174)

$$\frac{f_c}{G\ c_p} Pr^{2/3} = \frac{\zeta}{8} \qquad (10)$$

Until further data are made available the friction factor to be utilized in equation (10) probably should be that for smooth pipe, even when analyzing fairly rough tubes, for the extra pressure drop produced by roughness does not appear to yield a proportional increase in f_c. (See reference 7, p. 99.)

The dimples in the dimpled tube have an appreciable effect on the pressure drop, but only a small effect on the rate of heat transfer - for reasons other than the increased friction, as is discussed in a later paragraph. The question of the exact effect of roughness on the rate of heat transfer needs further clarification.

For the purpose of analysis, the friction factor of Nikuradse (reference 8) was utilized. For a range of the Reynolds modulus of 10,000 to 100,000 the equation of Nikuradse may be closely approximated (reference 9) by

$$\zeta = \frac{0.176}{Re^{0.200}} \tag{11}$$

Solving for f_c from equations (10) and (11) in terms of the physical properties of the gas*

$$f_c = 0.948 \times 10^{-4}(c_p{}^{0.333}\mu^{-0.467}k_a{}^{0.667})\frac{G^{0.80}}{D^{0.20}} \tag{12}$$

Plotting the group $(c_p{}^{0.333}\mu^{-0.467}k_a{}^{0.667})$ as a function of temperature and expressing the result as a power function of temperature allows the prediction of f_c at high gas temperatures. This procedure yields

$$f_c = 5.56 \times 10^{-4}\, T^{0.296}\frac{G^{0.80}}{D^{0.20}} \tag{13}$$

Equation (13) may be utilized directly to determine f_{ca}, using the inside diameter of the ventilating air tube for D. A question arises, however, concerning the value of D for the annular space. Recent investigations (references 11 and 12) show that the hydraulic diameter,** that is, $4 \times \frac{\text{cross-sectional area of flow}}{\text{wetted perimeter}}$, when utilized in the Reynolds number is a good criterion of the turbulence in the annulus. Substitution of this dimension in equation (13) will be found to yield satisfactory results.

Some recent data (references 12 and 15) indicate that an increase in f_{cg} is to be expected, owing to the "annulus effect." Because this correction is small

---

*The properties of air (reference 10) were utilized for both the ventilating air and the exhaust gases. This procedure for exhaust gases was resorted to in absence of more precise data; but it is probably sufficiently accurate since the exhaust gas is composed mainly of nitrogen, and combustion is complete.

**As contrasted to the quantity $4 \times \frac{\text{cross-sectional area}}{\text{heat-transfer perimeter}}$ which was suggested by Jordan (reference 13) and Nusselt (reference 14).

for the heater tested and there is a lack of agreement in the literature as to the exact value of the increase, this refinement was not included in the analysis. However, for exchangers in which the diameter of the outer surface of the annulus is much greater than the diameter of the air tube, this correction should not be overlooked.

Recapitulation

For prediction of the performance of simple gas-air, double tube heat exchangers the following equations are recommended:

$$\text{(a)}\quad q_a = \frac{\Delta t_{lm}}{\left[\frac{1}{(f_r + f_{cg})A_g} + \frac{1}{f_{ca}\, A_a}\right]} \qquad (14)$$

$$\text{(b)}\quad f_r = \frac{0.173\, F_A\, F_E \left[\left(\frac{T_w}{100}\right)^4 - \left(\frac{T_p}{100}\right)^4\right]}{(\tau_g - t_p)} \qquad (15)$$

$$\text{(c)}\quad f_{ca} = 5.56 \times 10^{-4}\, T_a^{0.296}\, \frac{G_a^{0.80}}{D_a^{0.20}} \qquad (16)$$

$$\text{(d)}\quad f_{cg} = 5.56 \times 10^{-4}\, T_g^{0.296}\, \frac{G_g^{0.80}}{D_g^{0.20}} \qquad (17)$$

The above equations were utilized to predict the rates of heat transfer for both the straight and dimpled tubes. This technique underestimates the dimpled-tube performance slightly. This discrepancy is discussed in a later paragraph.

SAMPLE CALCULATIONS

Run no. F-2 (Straight tube with mixing chamber)

Rate of air flow, W_a = 382 lb/hr

Rate of gas flow, W_g = 379 lb/hr

Inside diameter of air tube, $D_a = 0.149$ ft

Hydraulic diameter of gas annulus, $D_g = 0.0892$ ft

Heat transfer area, air side, $A_a = 2.23\ ft^2$

Heat transfer area, gas side, $A_g = 2.49\ ft^2$

Cross-sectional area of air flow, $0.0175\ ft^2$

Cross-sectional area of gas flow, $0.0295\ ft^2$

Air temperature entering, $\tau_{a_1} = 130^\circ$ F

Air temperature (mixed mean) leaving, $\tau_{a2} = 416^\circ$ F

Gas temperature, entering, $\tau_{g_1} = 1626^\circ$ F

Gas temperature, leaving, $\tau_{g2} = 1243^\circ$ F

(a) Calculation of the log mean temperature difference:

$$\Delta t_{lm} = \frac{(1626 - 130) - (1243 - 416)}{ln\left(\frac{1626 - 130}{1243 - 416}\right)} = 1135^\circ \text{ F}$$

(b) Calculation of f_{ca}

$$T_a = \frac{\tau_{a1} + \tau_{a2}}{2} + 460 = 733^\circ \text{ R}$$

$$G_a = \frac{W_a}{0.0175} = 21{,}800 \text{ lb/hr ft}^2$$

$$D_a = 0.149 \text{ ft}$$

$$f_{ca} = 5.56 \times 10^{-4}\, T_a^{0.296}\, \frac{G_a^{0.80}}{D_a^{0.20}}$$

$$= (5.56) \times 10^{-4} (733)^{0.296} \frac{(21800)^{0.80}}{(0.149)^{0.20}}$$

$$= 16.8 \text{ Btu/hr ft}^2\ ^\circ\text{F}$$

(c) Calculation of f_{cg}

$$T_g = \frac{\tau_{g1} + \tau_{g2}}{2} + 460 = 1895^\circ\ R$$

$$G_g = \frac{W_g}{0.0295} = 12{,}800\ \text{lb/hr ft}^2$$

$$D_a = 0.0892\ \text{ft}$$

$$f_{cg} = 5.56 \times 10^{-4}\ T_g^{\ 0.296}\ \frac{G_g^{\ 0.80}}{D_g^{\ 0.20}}$$

$$= 16.1\ \text{Btu/hr ft}^2\ {}^\circ F$$

(d) Calculation of f_r

The average temperature of the ventilating air tube (t_p) is required in order to calculate f_r.

$$q_a = f_{ca}\ A_a\ (t_p - \tau_a)$$

and

$$q_a \cong W_a\ c_p\ (\tau_{a2} - \tau_{a1})$$

Thus

$$t_p = \frac{W_a\ c_p}{f_{ca}\ A_a}\ (\tau_{a2} - \tau_{a1}) + \tau_a$$

$$= \frac{382 \times 0.241}{17.2 \times 2.23}\ (416 - 130) + 278$$

$$= 962^\circ\ F$$

Experimental data indicated that the average temperature along the outer surface of the exhaust gas annulus (t_w) was 250° F less than the arithmetic average gas temperature. Thus:

$$t_w = (\tau_g - 250) = 1435 - 250$$

$$= 1185^\circ\ F$$

The emissivity of oxidized steel is approximately (reference 2, p. 46) equal to 0.79

$$F_E = \frac{1}{\frac{1}{e_1} + \frac{A_g}{A_w}\left(\frac{1}{e_2} - 1\right)} = \frac{1}{\frac{1}{0.79} + \frac{2.49}{5.87}\left(\frac{1}{0.79} - 1\right)}$$

$$= 0.720$$

$$F_A = 1.00$$

Then

$$f_r = \frac{0.173 \times 0.720 \left[\left(\frac{1185 + 460}{100}\right)^4 - \left(\frac{962 + 460}{100}\right)^4\right]}{1435 - 962}$$

$$= 8.30$$

(e) Prediction of q_a

$$q_a = \frac{\Delta t_{lm}}{\left[\frac{1}{(f_r + f_{cg})A_g} + \frac{1}{f_{ca}\, A_a}\right]}$$

$$= \frac{1135}{\left[\frac{1}{(8.30 + 16.1)\ 2.49} + \frac{1}{16.8 \times 2.23}\right]}$$

$$= \frac{1135}{0.01645 + 0.0267}$$

$$= 26{,}300 \text{ Btu/hr}$$

The observed rate of heat transfer is:

$$q_M = W_a\, c_p\, (\tau_{a2} - \tau_{a1})$$

$$= 382 \times 0.241(416 - 130)$$

$$= 26{,}300 \text{ Btu/hr}$$

The ratio for this run is

$$\frac{q_a}{q_M} = \frac{26300}{26300} = 1.00$$

DISCUSSION OF RESULTS

The data and results are presented in table I.

Inspection of table I reveals that the rates of heat transfer predicted by means of equations (14), (15), (16), and (17) check the measured magnitudes for the straight tube with an average deviation of 6 percent. The average of the ratio of the predicted to the measured rates of heat transfer is 0.99. It should be noted that the change from the gasoline engine test stand to the natural gas test stand did not affect the accuracy of the results.

The equations (14), (15), (16), and (17) slightly underestimate the thermal capacity of the dimpled tube. The average of the ratio of predicted to measured rates of heat transfer for the dimpled tube is 0.925 with a mean deviation of ±3 percent.

It may be concluded from these results that the dimples increase the capacity of the dimpled tube about 7 percent, compared with the straight tube.

This increase is to be expected for several reasons. First, the dimples decrease the cross-sectional area of flow for the ventilating air. Equation (16) indicates an increase in f_{ca} owing to this change. Secondly, the dimples provide an increased surface area for heat transfer. Lastly, the dimples may increase the radiant heat transfer by acting as partial Hohlraums (ideal absorber).

Further inspection of table I shows that the radiant heat transfer from the outer wall of the gas annulus to the ventilating air tube was appreciable in the experiments. This condition, however, may not exist in actual installations where the outer wall of the annulus is at a lower temperature than existed in the laboratory. Thus the rates of heat transfer obtained in the laboratory are somewhat larger than may be expected under flight conditions for the same rates per unit area.

In order to help visualize the data presented in table I, a curve of

$$q_a = \frac{\Delta t_{lm}}{\left[\frac{1}{(f_r + f_{cg})A_g} + \frac{1}{f_a A_a}\right]} \tag{14}$$

is shown plotted in figure 6 as a function of the ventilating air rate per unit area for the following average experimental conditions for the straight tube:

Average gas temperature, $\tau_g = 1300^\circ$ F

Average air temperature, $\tau_a = 230^\circ$ F

Logarithmic temperature difference, $\Delta t_{lm} = 1050^\circ$ F

Unit conductance for radiation, $f_r = 7.0$ Btu/hr °F ft²

Weight rate of gas flow per unit area

Curve (1), $G_g = 13{,}000$ lb/hr ft²

Curve (2), $G_g = 26{,}000$ lb/hr ft²

For comparison with the predicted curves, data for several experimental runs are shown plotted in figure 6.

The data shown were corrected to a logarithmic mean temperature difference of 1050° F by multiplying the measured q_M by the ratio $\left(\frac{1050}{\Delta t_{lm}}\right)$ in order to allow direct comparison with the curves.

The rates of heat transfer to be expected at an exhaust gas rate of 26,000 lb/hr ft² are also shown. The increase is very small at low air rates, owing to high thermal resistance on the air side of the central tube.

A series of charts for the solution of equation (14) for rapid calculation of heater sizes (neglecting radiation) will be found at the end of the report.

TEMPERATURE DISTRIBUTION IN AIR STREAM

A very important point of experimental technique which has been overlooked by numerous investigators is the fact that, even at high magnitudes of the Reynolds modulus, a decided temperature gradient exists across an air stream being heated in a tube. That this must be the case may be demonstrated by an analysis of the thermal resistances from the tube wall to the center of the tube. It may be shown that (reference 5) the temperature distribution in the turbulent core is:

$$\frac{\Delta t}{\Delta t_{max}} = \frac{Pr + \ln(1 + 5\,Pr) + 0.5\,\ln \frac{Re}{60}\frac{y}{r_o}\sqrt{\frac{\zeta}{8}}}{Pr + \ln(1 + 5\,Pr) + 0.5\,\ln \frac{Re}{60}\sqrt{\frac{\zeta}{8}}} \qquad (18)$$

Integration of the temperature distribution across the tube yields:

$$\frac{\Delta t_{mean}}{\Delta t_{max}} = \frac{\int_o^{r_o} \frac{u}{u_{max}}\frac{\Delta t}{\Delta t_{max}}\, r\, dr}{\int_o^{r_o} \frac{u}{u_{max}}\, r\, dr} \qquad (19)$$

Utilizing the equation for the velocity distribution presented by Bakhmeteff (reference 16) gives the resulting ratio of $\frac{\Delta t_{mean}}{\Delta t_{max}}$ as shown in figure 7.

Figure 7 reveals that, unless a very excellent mixing chamber is utilized, a single measurement of temperature at the center of the air stream will introduce serious errors. Several runs were made purposely with no mixing chamber in order to demonstrate this point.

The data are shown in table II. The apparent temperature of the heated ventilating air in these runs was based on the readings of a single couple at the center of the air stream with no mixing chamber. In contrast to the satisfactory results shown in table I, the omission of the mixing chamber yielded apparent rates of heat transfer which were on the average 30 percent below the predicted values for the straight tube and 10 percent below the predicted values for the dimpled tube. The smaller discrepancy for the dimpled tube data is readily explained by a consideration of the temperature distribution which was measured across the tube diameter for the straight and dimpled tubes (fig. 8) during the tests. An inspection of these curves reveals that the dimples act as a partial mixing chamber for the dimpled tube temperature distribution curve is much flatter than that obtained in the straight tube. A comparison of the experimental curves and those predicted by equation (18) is shown. Application of equation (19) to the curves shown in figure 8 yields a ratio of $\frac{\Delta t_{mean}}{\Delta t_{max}} = 0.80$ for the straight tube and 0.90 for the dimpled tube, thus explaining the apparently greater temperature rise of the air passing through the dimpled tube.

A direct comparison of the experimental results shown in table II would lead to the erroneous conclusion that the dimpled tube was 30 percent more efficient than the straight tube, instead of the 7 percent improvement obtained by the more accurate mensuration of the exit air temperature.

PRESSURE DROP

The pressure drop along a tube in which a compressible fluid (gas) is being heated is not simply the frictional loss occurring along the tube, but also includes the effect of the expansion of the gas as it becomes heated. The latter effect produces a large fraction of the total pressure drop, so that pressure losses observed under nonisothermal conditions should be corrected to isothermal conditions - or, preferably, isothermal pressure drops should be observed if the frictional loss through the heater is desired directly.

The analysis of the nonisothermal pressure drop through a cylindrical tube of constant diameter is presented below.

The Bernoulli equation for a horizontal tube is:

$$\frac{dP}{\gamma} + \frac{v\,dv}{g} + \zeta \frac{v^2}{2g} \frac{dx}{D} = 0 \qquad (20)$$

For a constant weight rate there is a definite relation between velocity and density. Thus,

$$v = \frac{\frac{G}{3600}}{\gamma}$$

or

$$\gamma = \frac{G}{3600\ v} \qquad (21)$$

Thus the Bernoulli equation becomes

$$\int_1^2 dP + \int_1^2 \frac{G}{3600}\frac{dv}{g} = -\zeta \frac{G}{3600}\frac{1}{2gD}\int_0^N v\ dx \qquad (22)$$

By assumption of a linear increase of velocity* with length due to heating of the fluid, the velocity at entrance to the heating section is v_1, and at exit $v_1\left(\frac{T_2}{T_1}\right)$. Thus at any point x along the heating length,

$$v = v_1 + v_1\left(\frac{T_2}{T_1} - 1\right)\frac{x}{N} \qquad (23)$$

where T_1 and T_2 are the absolute mixed mean temperatures of the fluid entering and leaving the heating section.

Substituting the above equation in the Bernoulli expression and integrating** yields:

$$(P_1 - P_2) + \frac{G}{3600\ g}(v_1 - v_2) = \zeta_{T_a}\frac{G}{3600}\frac{v_1}{2gD}\left(\frac{T_1 + T_2}{2T_1}\right)N \qquad (24)$$

Substituting

$$v_1 = \frac{G}{3600\ \gamma_1}$$

*The increase in velocity is actually exponential, but as a first approximation a linear variation may be utilized.

**Assuming ζ to be constant. Actually ζ varies slightly with length due to the change in Reynolds modulus as the fluid becomes heated.

$$v_2 = \frac{G}{3600 \ \gamma_2}$$

$$\frac{\gamma}{\gamma_2} = \frac{T_2}{T_1} \quad \text{and} \quad \frac{T_1 + T_2}{2} = T_a$$

yields

$$\zeta_{T_a} \frac{G^2}{(3600)^2 2g \ \gamma_1} \frac{N}{D} = \left(\frac{T_1}{T_a}\right) \left[(P_1 - P_2) - \frac{G^2}{(3600)^2 \gamma_1 g} \left(\frac{T_2}{T_1} - 1\right) \right] \tag{25}$$

To obtain the isothermal head loss at the temperature T_1, the friction factor ζ_{T_a} must be replaced by the friction factor calculated at the temperature T_1 (ζ_{T_1})

The friction factor (reference 9) usually is expressed as:

$$\zeta_T = \frac{C}{\left(\frac{G \ D}{3600 \ g \ \mu_T}\right)^{0.20}}$$

but (reference 10)

$$\mu_T \ \alpha \ T^{2/3}$$

Thus

$$\zeta_{T_a} = \zeta_{T_1} \left(\frac{T_a}{T_1}\right)^{0.13}$$

Thus the final equation becomes:

$$\left(\zeta_{T_1} \frac{G^2}{(3600)^2 \ 2g \ \gamma_1} \frac{N}{D}\right)$$

$$= \left(\frac{T_1}{T_a}\right)^{1.13} \left[(P_1 - P_2) - \frac{G^2}{(3600)^2 \ \gamma_1 \ g} \left(\frac{T_2}{T_1} - 1\right) \right] \tag{26}$$

where

$$\left(\zeta_{T_1} \frac{G^2}{(3600)^2 \, 2g \, \gamma_1} \frac{N}{D}\right) = \Delta P_{T_1},$$ the isothermal pressure drop due to friction at temperature T_1

A similar derivation is presented by McAdams (reference 2, p. 130).

Thus the isothermal head loss due to friction, based on the temperature T_1 is equal to the measured non-isothermal head loss $(P_1 - P_2)$ less a correction

$$\frac{G^2}{(3600)^2 \, \gamma_1 \, g}\left(\frac{T_2}{T_1} - 1\right)$$ and is multiplied by the ratio

$$\left(\frac{T_a}{T_1}\right)^{1.13}$$. Conversely, if the isothermal head loss is known, the nonisothermal loss may be calculated.

$$(P_1 - P_2) = \Delta P_{T_1}\left(\frac{T_a}{T_1}\right)^{1.13} + \frac{G^2}{(3600)^2 \, \gamma_1 \, g}\left(\frac{T_2}{T_1} - 1\right) \qquad (27)$$

It should be noted that the nonisothermal head loss is greater than the isothermal for a fluid heating, but less for a fluid cooling.

Several runs were made in order to check the validity of the derivation shown above.

The data and results are shown in tables III and IV, and are plotted in figures 9 and 10. A series of runs was made to obtain the isothermal pressure drops (table III), and another set of data obtained under nonisothermal (heating) conditions (table IV).

Inspection of figures 9 and 10 reveals that for both tubes the pressure drop* during the nonisothermal conditions is, roughly, twice that during isothermal conditions.

---

*The pressure drop per foot is plotted for convenience, but it should be remembered that this value is only an <u>average</u>, for the pressure drop will not be a linear function of length due to heating of the ventilating air.

Application of equation (26) reveals that this discrepancy is due largely to the effect of the reduction of the air density upon heating, and the resulting increase in fluid velocity. Some of the increased pressure drop is due also to the increased air viscosity in the laminar sublayer (reference 5).

Equation (26) was utilized to predict the isothermal pressure drop from the nonisothermal, as follows:

(a) The quantity,

$$\Delta P_{T_1} = \left(\frac{T_1}{T_a}\right)^{1.13} \left[(P_1 - P_2) - \frac{G^2}{(3600)^2\ \gamma_1\ g}\left(\frac{T_2}{T_1} - 1\right)\right]$$

was computed. This magnitude is the isothermal pressure drop to be expected if the air passing through the heater is at the temperature T_1.

(b) From equation (26) it is noted that, if the isothermal pressure drop at any other temperature T is desired,

$$\frac{\Delta P_T}{\Delta P_{T_1}} = \left(\frac{\zeta_T\ \gamma_1}{\gamma_T\ \zeta_{T_1}}\right) = \left(\frac{T}{T_1}\right)^{1.13} \tag{28}$$

For direct comparison to the isothermal data which were obtained at 78° F all the magnitudes of ΔP_{T_1} were corrected to 78° F by means of equation (28).

The isothermal pressure drops computed in this manner from the nonisothermal data checked the measured values within 27 percent for the straight tube and 7 percent for the dimpled tube. Thus, equation (26) appears to be reasonably successful in correlating the isothermal and nonisothermal pressure drops in tubular heat exchangers.

As a further comparison, the isothermal friction factors for the dimpled and straight tubes are compared to the smooth pipe data of McAdams (reference 2, p. 172) and Nikuradse (reference 8) in figure 11. The magnitudes of the friction factor for the straight tube lie somewhat above the smooth pipe curve. The friction factor for the dimpled tube is about 1.6 times that for the smooth tube. This increase is to be expected because of the effect of the dimples.

On the gas side of the exchangers the following average nonisothermal pressure drops were observed for a gas rate of 420 lb/hr.

Nonisothermal Pressure Drop

	$\frac{lb/ft^2}{ft}$	T_{g_1}	T_{g_2}
Straight tube	2.62	1500° F	1000° F
Dimpled tube	3.24	1500° F	1000° F

The isothermal pressure drop would be somewhat greater, as is shown by equation (26).

CONCLUSIONS

1. The data presented in this section indicate that for testing the thermal output and the pressure drop performance of double tube heat exchangers, hot gases produced by a natural gas burner yield results substantially similar to engine exhaust gases.

2. Equations (14), (15), (16), and (17) are applicable to the predictions of the rates of heat transfer in double tube heat exchangers (exhaust gas to air).

3. The dimpled-type tube shows a slight advantage (7 percent) in heat capacity over the straight tube.

4. Unless a well-designed mixing chamber is utilized at the point where the temperature of a nonisothermal gas stream is measured, appreciable errors will result in the measured temperature.

5. The nonisothermal pressure drop along a tube in which a gas flows differs widely from the isothermal friction loss. Equation (26) allows the prediction of the isothermal loss from the nonisothermal and equation (27) may be utilized to calculate the nonisothermal pressure drop when the isothermal is known.

6. The isothermal friction factor for the dimpled tube is 1.6 times that for the straight tube. The latter is somewhat greater than the friction factor for smooth pipe.

University of California,
Berkeley, Calif.

APPENDIX

In order to facilitate the quick estimate of the heating capacity of any double tube heat exchanger, a series of charts have been drawn which allow the graphical determination of heater capacities. These charts are based on equations (14), (16), and (17). Radiant heat transfer is omitted.

Chart A allows the determination of the log mean temperature difference Δt_{lm} when the terminal temperature differences are known.

Chart B allows the determination of the thermal resistance of the heater per foot of length $\left(\frac{1}{f_cP}\right)_a \left(\frac{1}{f_cP}\right)_g$, when the rates of gas flow, air flow, and the cross-sectional design of the heater are known.

The thermal output of a given heater q_a or the of heater required to give a certain output N may be determined from the simple equation

$$q_a = \frac{\Delta t_{lm} \times N}{\left[\left(\frac{1}{f_cP}\right)_a + \left(\frac{1}{f_cP}\right)_g\right]} \tag{A1}$$

where

N length of heat exchanger, ft

P heat-transfer perimeter, ft

An example is presented to clarify the use of the charts.

Example

Given a heater with the cross section shown in fig. 12.

The heater is 3 ft long. The following design conditions are assumed:

Rate of exhaust gas flow . . . . 6000 lb/hr

Rate of ventilating air flow . . . . 2000 lb/hr

Temperature of exhaust gas entering heater . . . . 1600° F

Temperature of exhaust gas leaving heater . . . . 1100° F

Temperature of air entering heater . . . . . . -60° F

Temperature of air leaving heater . . . . . 400° F

To determine:

1. The output of the heater if the air flows in the spaces marked A in fig. 12, and the exhaust gases in the central space (B, C).

2. The output of the heater if the flow is the same as under 1, but the central 3-inch hole (C) is closed off.

3. The output of the heater if the air flows in the spaces marked B and the exhaust gases through A.

4. The average temperature of the heat transfer surface under the above conditions.

Notes: 1. Pressure drop and manifolding design considerations have been neglected. These, of course, may invalidate some of the combinations proposed above.

2. The assumed temperatures will change with the heater output, but as a first approximation, the temperatures will be considered unchanged.

Solution

From fig. 12 the following data are obtained:

TABLE V.- HEATER DATA

	Proposal (1)	Proposal (2)	Proposal (4)
Cross-sectional area of air flow (sq in.)	31.4	31.4	11.8
Cross-sectional area of gas flow (sq in.)	18.9	11.8	31.4
Wetted perimeter of air flow (in.)	105	105	89
Wetted perimeter of gas flow (in.)	80	89	105
Heat-transfer perimeter for air (in.)	80	80	80
Heat-transfer perimeter for gas (in.)	80	80	80

The average gas temperature is 1350° F. The average air temperature is 170° F. The temperature differences between gas and air are:

At entrance $\Delta t_1 = 1660^\circ$ F

At exit $\Delta t_2 = 700^\circ$ F

From chart A:

At $\Delta t_1 = 1660^\circ$ F, $\Delta t_2 = 700^\circ$ F, $\Delta t_{lm} = 1100^\circ$ F

From chart B, entering with the weight rate of air or exhaust gas flow, and proceeding as shown by the dotted line, the following values are obtained:

TABLE VI.- THERMAL RESISTANCES FROM CHART B

	Proposal (1)	Proposal (2)	Proposal (3)
$\left(\frac{1}{f_c P}\right)_{air}$ $\frac{^{o}F}{(Btu/hr\ ft)}$	0.0175	0.0175	0.0062
$\left(\frac{1}{f_c P}\right)_{gas}$ $\frac{^{o}F}{(Btu/hr\ ft)}$	.0034	.0020	.0053
$\left[\left(\frac{1}{f_c P}\right)_{air} + \left(\frac{1}{f_c P}\right)_{gas}\right]$	.0209	.0195	.0115

Substituting in equation (A1) for a heater length of $N = 3$ ft:*

$$q_a = \frac{\Delta t_{lm} N}{\left[\left(\frac{1}{f_c P}\right)_a + \left(\frac{1}{f_c P}\right)_g\right]}$$

Proposal (1) $\quad q_a = 157,000$ Btu/hr

Proposal (2) $\quad q_a = 169,000$ Btu/hr

Proposal (3) $\quad q_a = 287,000$ Btu/hr

Inspection of table VI reveals that when the gas flows in the B spaces and the air in the A spaces, the thermal resistance on the air side is so large that the heater capacity is low. Closing off the central hole has little effect on the heater capacity. But, by reversing the position of the air and the gas (proposal 3) the two thermal resistances are equalized and the heater capacity is practically doubled. The optimum condition for heat transfer normally would be one in which the air and the gas side resistances are about equal.

*For more accurate calculations the log mean temperature difference Δt_{lm} should be recalculated to agree with the thermal output of the heater.

Chart B may be used to design for this condition. If the length of heater at capacity and the log mean temperature difference are fixed, the total resistance

$$\left(\frac{1}{f_c P}\right)_a + \left(\frac{1}{f_c P}\right)_g$$ may be determined. One-half of this

total resistance will be the desired resistance on the gas or the air side. Utilizing chart B, by choosing various combinations of cross-sectional areas and perimeters, a heater may be evolved with the desired characteristics.

The average temperature of the heat-transfer surface also may be estimated. By analogy to electrical circuits (reference 17) the average temperature of the heat-transfer surface may be estimated from the resistances shown in table VI.

Thus for proposal (1)

Total resistance	0.0209 $\frac{^{\circ}F}{Btu/hr\ ft}$
Gas side resistance	0.0034 $\frac{^{\circ}F}{Btu/hr\ ft}$
Average gas temperature	1350° F
Average air temperature	170° F
Difference	1800° F

Thus the drop in temperature from the gas to the tube wall is

$$T_g - t_p = \frac{0.0034}{0.0209} \times 1180 = 192^{\circ}\ F$$

or $$t_p = 1350 - 192 = 1158^{\circ}\ F$$

In a similar manner for

Proposal (2) $t_p = 1229^{\circ}$ F

Proposal (3) $t_p = 805^{\circ}$ F

Thus, the proper proportioning of the thermal resistances on the air and gas side not only improved the heater capacity, but lowered the temperatures of the heat transfer surface over 400° F.

The foregoing method, however, will not reveal local high temperature conditions which may exist in a heater because of improper design of entrance conditions, manifolding, etc.

The above example was selected to illustrate the use of the charts and is not to be considered a suggested design.

The authors wish to express appreciation to Messrs. H. F. Brockscmidt, M. Tribus, D. Dubain, M. A. Miller, and F. Hamaker for their help in the performance of the tests and the preparation of the report, and to Messrs. H. Eagles and H. Poeland for constructing the laboratory equipment.

REFERENCES

1. Subcommittee on Exhaust Gas Temperature Measurement of the A.S.M.E. Committee on Industrial Instruments and Regulators: Exhaust Gas Temperature Measurement. Proposed Standardized Instrumentation and Procedure. Sept. 1941.

2. McAdams, Wm. H.: Heat Transmission. McGraw-Hill Book Co., Inc., 1933.

3. Hottel, H. C., and Egbert, R. B.: The Radiation of Furnace Gases. Trans. A.S.M.E., May 1941, p. 297.

4. Boelter, L. M. K.: Supplementary Heat Notes. Univ. of Calif. Press, 3d ed., 1942, p. XIV-1.

5. Boelter, L.M.K., Martinelli, R. C., and Jonassen, Finn: Remarks on the Analogy between Heat Transfer and Momentum Transfer. Trans. A.S.M.E. July 1941, p. 447.

6. Colburn, A. P.: A Method of Correlating Forces Convection Heat Transfer Data and a Comparison with Fluid Friction. Trans., Am. Inst. Chem. Eng., vol. XXIX, 1933, p. 174.

7. Cope, W. F.: Proc. Inst. Mech. Eng. (London), vol. 145, 1941, p. 99.

8. Rouse, H.: Fluid Mechanics for Hydraulic Engineers. Eng. Soc. monograph. McGraw-Hill Book Co., Inc., 1938, p. 249.

9. Ludin, B.: Special Course Report, Course Mech. Eng. 131B, Univ. of Calif.

10. Tribus, Myron, and Boelter, L. M. K.: An Investigation of Aircraft Heaters. II - Properties of Gases. NACA A.R.R., Oct. 1942.

11. Wiegand, J. H., and Baker, E. M.: Transfer Processes in Annuli. Trans Am. Inst. Chem. Eng., June 25, 1941, p. 569.

12. Monrad, C. C., and Pelton, J. F.: Heat Transfer by Convection in Annular Spaces. Trans. Am. Inst. Chem. Eng., June 25, 1941, p. 593.

13. Jordan, H. P : On the Rate of Heat Transmission between Fluids and Metal Surfaces. Proc. Inst. Mech. Eng. (London) Dec. 1909, pts. 3-4, p. 1317.

14. Nusselt, W.: Z.V.D.I., vol. 57, 1913, p. 199.

15. Foust, A. S., and Christian, G. A.: Trans. Am. Inst. Chem. Eng., vol. 36, 1940, p. 541.

16. Bakhmeteff, B. A.: The Mechanics of Turbulent Flow, Princeton Univ. Press, 1936, p. 80.

17. Martinelli, R. C., Tribus, M., and Boelter, L. M. K.: An Investigation of Aircraft Heaters. I - Elementary Heat Transfer Considerations in an Airplane. NACA A.R.R., Oct. 1942.

TABLE I. TABULATED RESULTS AND DATA

Run	G_a $\left(\frac{lb}{hr\ ft^2}\right)$	G_g $\left(\frac{lb}{hr\ ft^2}\right)$	τ_{a1} (°F)	τ_{a2} (°F)	τ_{g1} (°F)	τ_{g2} (°F)	Calculated t_p (°F)	f_{ca} $\left(\frac{Btu}{hr\ ft^2\ °F}\right)$	f_{cg} $\left(\frac{Btu}{hr\ ft^2\ °F}\right)$	f_r $\left(\frac{Btu}{hr\ ft^2\ °F}\right)$	q_a (Btu/hr)	q_M (Btu/hr)	Ratio $\frac{q_a}{q_M}$
	Straight tube . . . . Mixing chamber . . . (gasoline engine)												
C-1	26,800	15,600	106	304	1340	932	720	19.6	17.6	3.8	21,850	22,250	0.981
C-2	21,000	15,600	108	324	1341	952	741	16.3	17.6	3.5	19,600	19,100	1.025
C-3	18,400	15,800	106	328	1341	954	743	14.5	18.4	3.8	18,600	17,100	1.088
C-4	17,000	15,500	105	338	1323	952	770	13.7	18.0	3.2	17,300	16,700	1.035
	Straight tube . . . . Mixing chamber . . . (natural gas)												
F-1	27,100	13,400	123	392	1627	1203	951	20.2	16.7	8.2	29,000	30,800	0.940
F-2	21,800	12,800	130	416	1626	1243	964	16.9	16.1	8.3	26,300	26,300	1.000
F-3	18,300	12,950	102	417	1629	1241	979	14.7	16.2	8.5	24,400	23,590	1.03
F-4	14,400	12,100	106	416	1624	1184	954	12.1	15.5	7.7	20,200	18,750	1.08
F-5	14,500	13,500	104	391	1502	1114	894	12.2	16.4	6.1	18,700	17,500	1.07
F-6	19,100	13,500	108	377	1497	1109	883	15.1	16.4	6.2	21,700	21,580	1.005
F-7	20,100	13,400	113	371	1496	1093	857	15.8	16.6	7.5	22,700	21,800	1.04
F-8	27,700	13,500	127	336	1490	1030	758	20.4	16.4	6.3	25,200	24,400	1.03
F-9	16,900	14,100	95	332	1293	941	762	13.8	16.5	4.5	17,000	16,900	1.005
F-10	19,100	14,100	105	323	1291	939	740	14.9	16.5	4.3	17,600	17,600	1.00
F-11	21,700	14,100	109	315	1299	939	721	16.6	16.5	4.4	19,200	18,800	1.02
F-12	27,600	14,100	124	302	1297	917	675	20.1	16.5	4.4	21,100	20,700	1.02
F-13	30,500	13,100	83	313	1609	1089	823	21.6	16.2	6.7	28,900	29,500	.980
F-14	32,500	12,600	82	337	1620	1216	892	23.0	15.9	8.4	30,000	34,900	.860
F-15	36,400	12,600	82	318	1609	1184	856	24.8	15.9	8.5	33,800	36,300	.932
F-16	36,600	13,600	82	248	1508	926	623	24.8	16.1	4.1	24,300	25,300	.962
F-17	32,400	13,900	76	265	1295	909	690	22.4	16.1	3.8	22,400	26,000	.862
F-18	16,700	13,250	77	287	1313	956	688	13.2	15.9	4.2	16,800	14,900	1.13
F-19	32,400	12,800	71	312	1516	1059	858	22.4	15.9	6.5	28,000	33,400	.840
F-20	36,200	12,800	78	309	1513	1070	829	24.9	15.9	6.6	29,600	35,200	.840
	Dimpled tube . . . . Mixing chamber . . . (natural gas)												
H-1	18,600	13,850	101	315	1290	892	754	14.5	16.2	3.3	17,000	18,500	0.918
H-2	20,600	13,950	104	312	1296	905	750	15.6	16.4	3.5	18,100	19,850	.912
H-3	26,400	14,400	111	279	1299	839	667	18.9	16.6	3.7	19,700	20,850	.944
H-4	18,100	13,150	111	379	1515	1043	885	14.0	16.1	5.3	19,800	22,590	.878
H-5	20,300	13,600	112	359	1515	1021	874	15.6	16.6	5.5	21,800	23,200	.940
H-6	25,600	13,800	119	337	1516	1013	838	18.8	16.6	5.5	24,500	26,800	.915
H-7	18,200	13,100	119	402	1604	1101	941	14.5	16.3	7.0	22,200	23,100	.962
H-8	20,500	13,200	121	389	1607	1100	921	15.8	16.1	7.1	23,700	24,300	.977
H-9	26,200	13,250	126	360	1610	1071	1043	19.2	16.1	7.0	26,400	29,590	.894
H-10	30,600	13,400	83	240	1302	859	642	21.0	15.8	3.8	21,800	23,700	.918
H-11	34,400	13,250	84	232	1295	866	652	22.8	15.8	3.8	22,900	26,400	.867
H-12	34,400	12,950	86	266	1510	966	702	22.8	15.8	5.9	27,500	28,100	.980
H-13	35,400	12,500	89	286	1607	1032	771	23.6	15.6	7.4	30,700	32,400	.948

TABLE II.- DATA AND RESULTS WITH NO MIXING CHAMBER

Run	G_a (lb / hr ft²)	G_g (lb / hr ft²)	T_{a1} (°F)	T_{a2} (°F)	T_{g1} (°F)	T_{g2} (°F)	Calculated t_p (°F)	f_{ca} (Btu / hr ft² °F)	f_{cg} (Btu / hr ft² °F)	f_r (Btu / hr ft² °F)	q_a (Btu / hr)	q_M (Btu / hr)	Ratio q_a/q_M
	Straight tube - No mixing chamber												
G-1	38,500	14,500	75	188	1308	861	454	25.6	16.7	4.1	24,850	18,300	1.36
G-2	39,000	13,500	75	204	1519	983	522	25.6	16.3	5.9	32,000	21,180	1.51
G-3	33,100	13,300	77	228	1508	1021	569	22.6	16.1	6.3	28,550	21,000	1.36
G-4	30,100	13,200	77	239	1523	1040	594	20.8	16.1	6.6	27,700	20,400	1.36
G-5	16,500	12,900	95	306	1612	1133	696	13.2	16.0	8.1	22,500	14,600	1.54
G-6	20,700	12,700	100	303	1604	1173	556	16.0	15.8	7.8	26,100	17,520	1.49
G-7	23,900	12,700	106	302	1597	1174	702	17.9	15.8	8.4	27,600	19,900	1.38
G-8	30,100	12,700	116	277	1591	1133	623	21.2	15.8	7.7	29,600	20,200	1.46
G-9	34,300	12,900	84	240	1611	1121	592	23.6	16.0	7.7	32,700	22,400	1.46
G-10	40,300	12,900	84	227	1614	1121	562	26.6	16.0	7.5	35,000	24,200	1.44
	Dimpled tube - No mixing chamber												
I-1	19,800	13,100	96	277	1290	876	657	14.7	15.4	3.4	17,100	16,600	1.03
I-2	21,500	13,100	98	265	1297	862	634	15.3	15.4	3.6	18,050	17,720	1.02
I-3	28,200	13,100	112	248	1297	849	565	19.8	15.3	3.8	20,300	17,800	1.14
I-4	20,200	12,800	110	327	1512	1011	773	15.6	15.6	5.8	19,900	20,200	.986
I-5	20,900	12,600	109	318	1513	1011	756	16.0	15.4	5.9	22,400	20,300	1.10
I-6	29,000	12,800	120	292	1523	986	706	20.6	15.5	7.7	26,500	23,150	1.14
I-7	20,100	12,500	107	347	1602	1091	830	15.5	15.7	7.2	23,800	21,900	1.09
I-8	21,000	12,400	110	346	1594	1101	814	16.1	15.5	7.3	24,400	22,100	1.10
I-9	28,500	12,400	121	314	1607	1071	774	19.5	15.4	7.3	27,400	25,400	1.08
I-10	34,900	12,600	84	232	1604	1022	601	23.2	15.6	7.0	30,600	24,000	1.27

TABLE III.- ISOTHERMAL PRESSURE DROP - AIR SIDE

Run	W_a (lb/hr)	G_a $\left(\frac{lb}{hr\ ft^2}\right)$	T_1 (°F)	Measured pressure drop $\left(\frac{lb/ft^2}{ft}\right)$	Reynolds number	Friction factor
Straight tube (distance between pressure taps, 6.16 ft)						
KIS-1	394	22,500	78	1.47	75,400	0.0269
KIS-2	411	23,500	78	1.64	78,900	.0272
KIS-3	561	32,100	78	2.58	107,500	.0229
KIS-4	631	36,100	78	3.14	121,000	.0221
KIS-5	681	38,900	78	3.33	130,000	.0200
Dimpled tube (distance between pressure taps, 6.21 ft)						
KID-1	670	34,600	78	4.42	122,000	0.0354
KID-2	617	32,200	78	3.84	113,000	.0354
KID-3	525	27,200	78	2.93	96,000	.0382
KID-4	456	23,600	97	2.48	81,100	.0412
KID-5	408	21,200	97	2.18	73,000	.0448

W-98

TABLE IV. NON ISOTHERMAL PRESSURE DROP

Air side

Run	W_a (lb/hr)	G_a $\left(\frac{lb}{hr\ ft^2}\right)$	Measured non isothermal pressure drop (lb/ft²)	T_1 (°R)	T_2 (°R)	T_a (°R)	Non isothermal pressure loss* (lb/ft²)	Non isothermal pressure loss per foot** (lb/ft²/ft)	Measured non isothermal pressure loss (lb/ft²/ft)
	Straight tube	(Distance between pressure taps, 6.16 ft)							
K-1	355	20,300	19.7	563	823	692	10.5	1.62	3.20
K-2	398	22,750	23.4	564	815	668	12.8	1.97	3.77
K-3	503	28,700	32.8	572	798	683	17.5	2.66	5.33
K-4	578	33,000	41.0	545	750	647	22.6	3.64	6.66
K-5	685	39,100	51.2	545	738	640	27.8	4.47	8.32
	Dimpled tube	(Distance between pressure taps, 6.21 ft)							
L-1	348	19,900	22.1	560	883	721	12.0	1.85	3.56
L-2	389	22,200	26.2	567	880	723	13.9	2.14	4.22
L-3	528	30,200	40.1	578	844	711	22.0	3.38	6.46
L-4	688	39,300	49.6	553	737	645	29.7	4.57	7.99
L-5	610	34,900	42.6	552	745	648	25.8	3.98	6.86

*Corrected to isothermal condition at T_1 (See equation 26.)

**Corrected to isothermal condition at 78° F (See p. 23.)

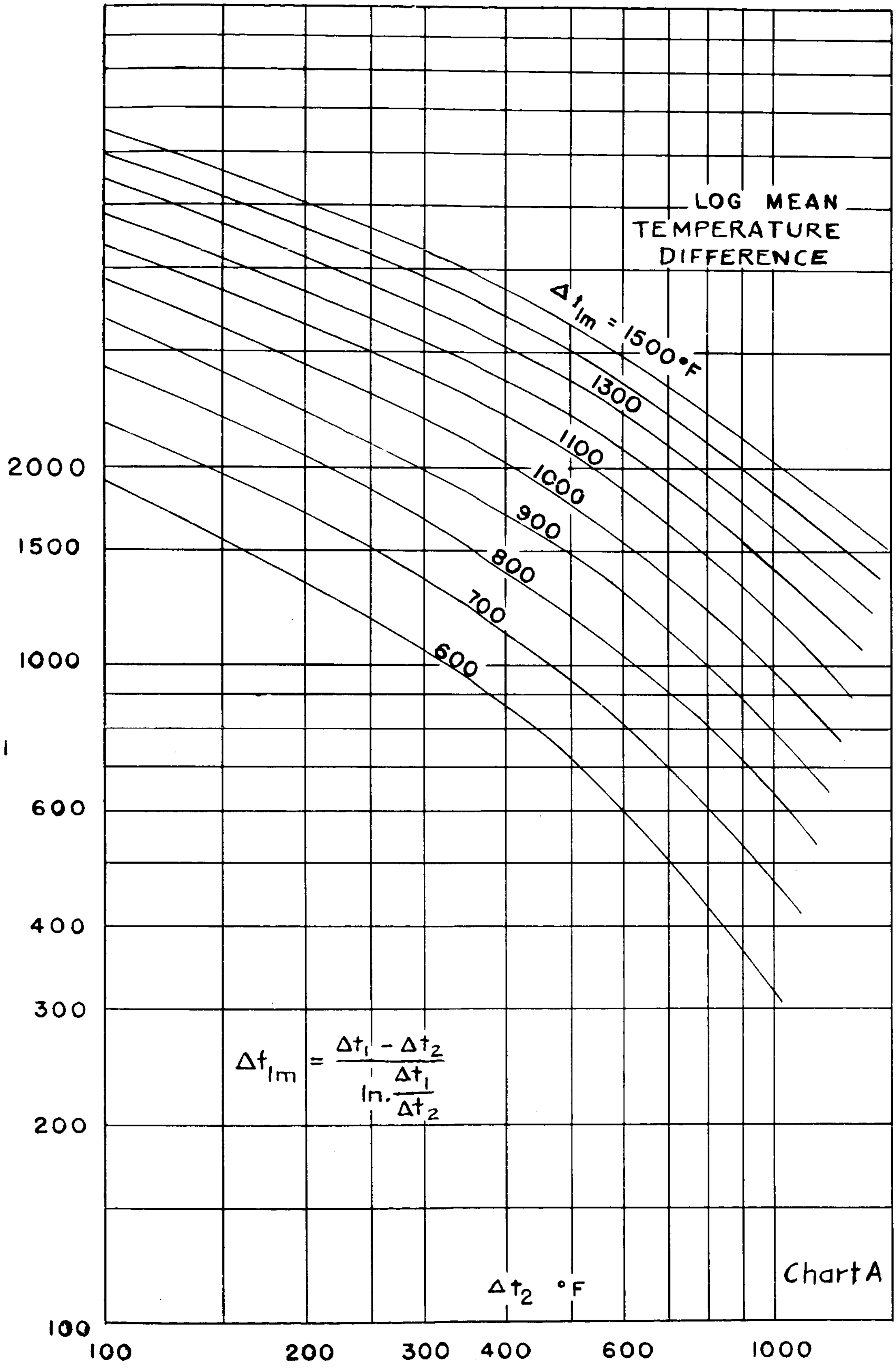
LOG MEAN
TEMPERATURE
DIFFERENCE
Δt lm = 1500°F
1300
1100
1000
900
800
700
600
2000
1500
1000
Δt1
°F
600
400
300
200
100
$$\Delta t_{lm} = \frac{\Delta t_1 - \Delta t_2}{\ln \frac{\Delta t_1}{\Delta t_2}}$$
Δt2 °F
100
200
300
400
600
1000
Chart A

W-98

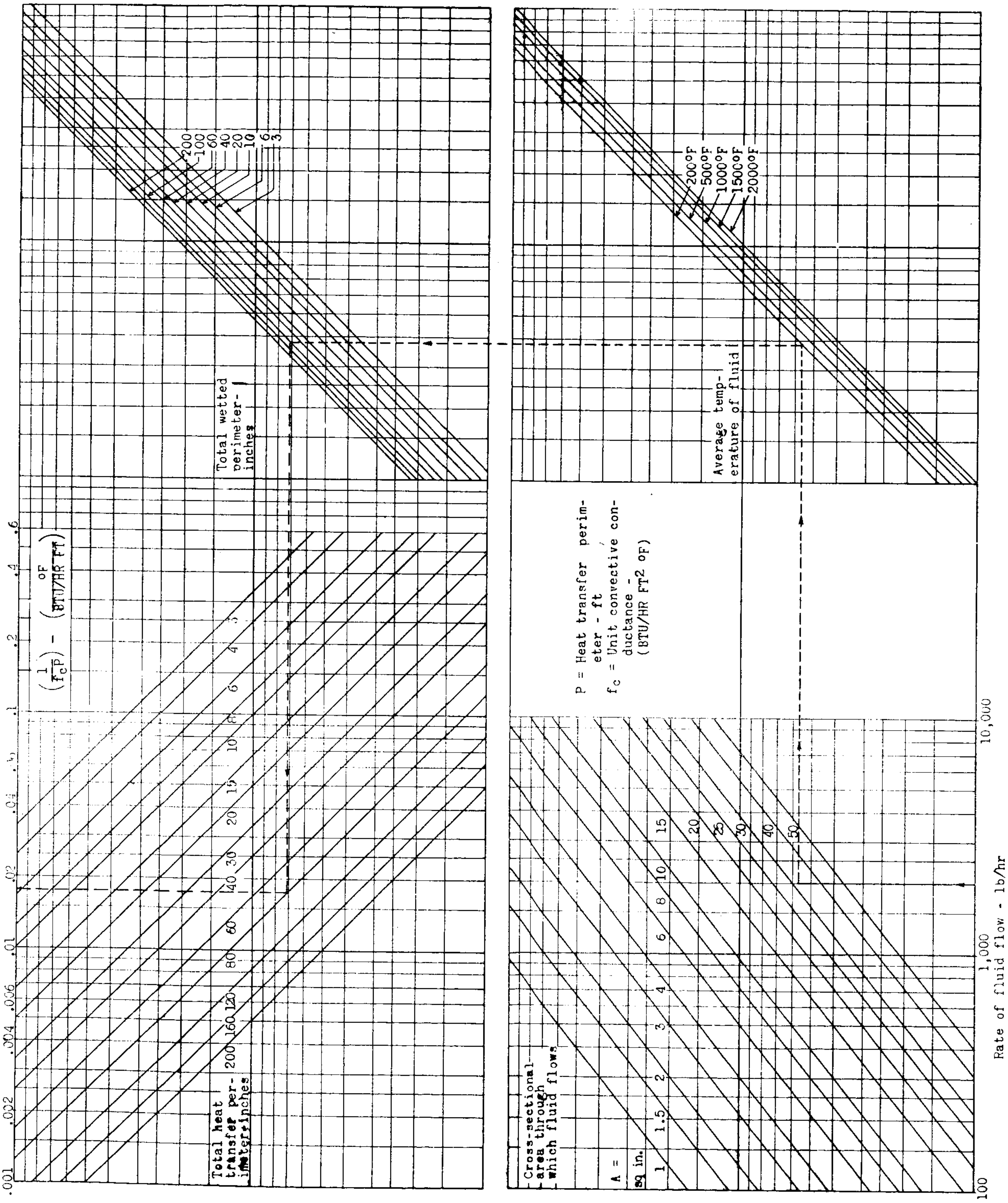
Total wetted perimeter- inches
200
100
60
40
20
10
6
3
200°F
500°F
1000°F
1500°F
2000°F
Average temp- erature of fluid
P = Heat transfer perim- eter - ft
f_c = Unit convective con- ductance - (BTU/HR FT2 °F)
(1/f_cP) - (°F/BTU/HR FT)
.001
.002
.004
.006
.01
.02
.1
.2
.4
.6
Total heat transfer per- imeter - inches
200
160
120
80
60
40
30
20
15
10
8
6
4
3
Cross-sectional area through which fluid flows
A = sq in.
1
1.5
2
3
4
6
8
10
15
20
25
30
40
50
100
1,000
10,000
Rate of fluid flow - lb/hr

Chart B

W-98

TEST STATION FOR GAS - AIR HEAT EXCHANGERS

SCHEMATIC DIAGRAM

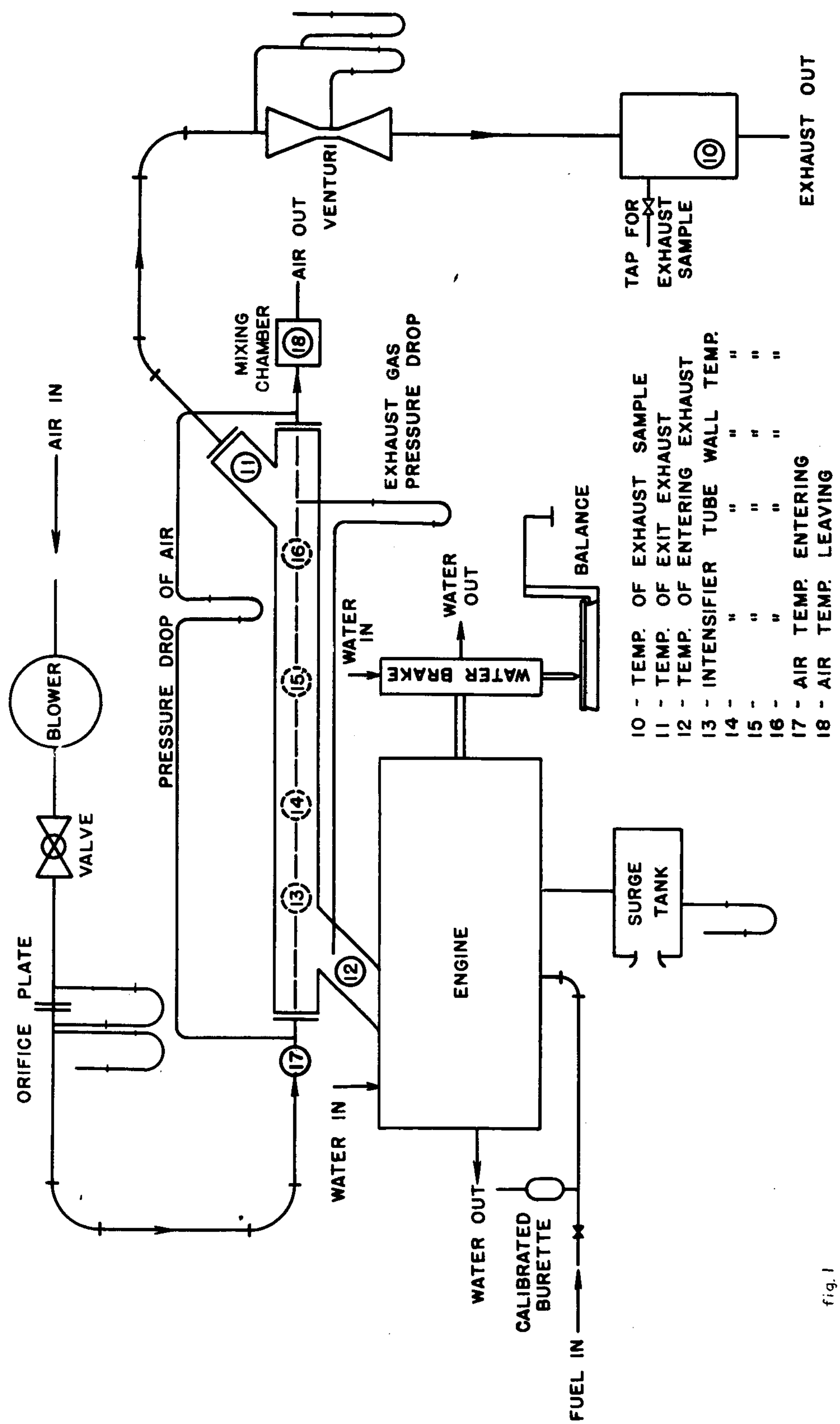

fig. 1

TEST STATION FOR GAS-AIR HEAT EXCHANGERS

SCHEMATIC DIAGRAM

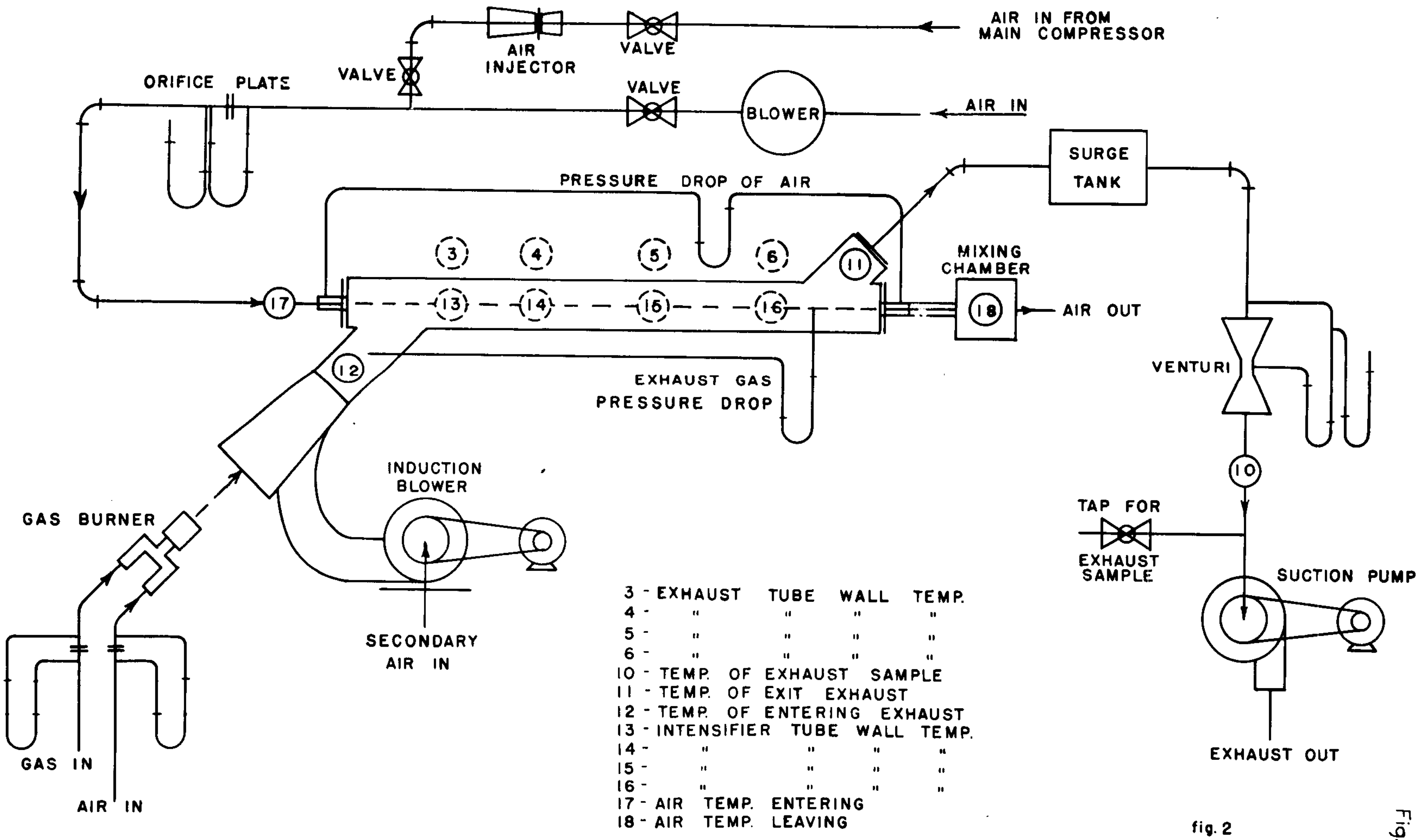

fig. 2

Fig. 2

STRAIGHT TUBE

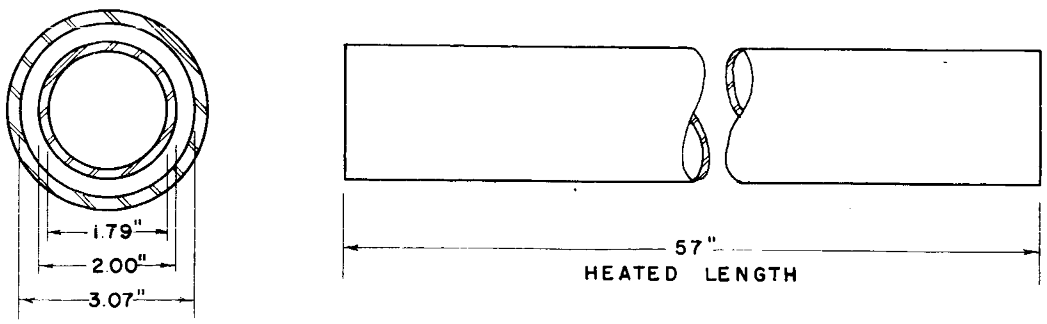

CROSS - SECTIONAL AREAS
AIR SIDE = 0.0175 ft^2
GAS SIDE = 0.0295 ft^2

HEAT - TRANSFER AREAS
AIR SIDE (A_a) = 2.23 ft^2
GAS SIDE (A_g) = 2.49 ft^2

HYDRAULIC DIAMETERS
AIR SIDE (D_a) = 0.149 ft.
GAS SIDE (D_g) = 0.0892 ft.

fig. 4

DIMPLED TUBE

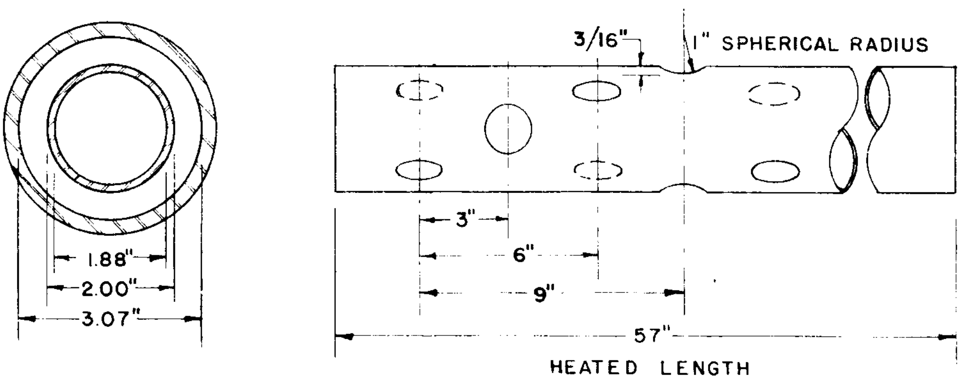

CROSS-SECTIONAL AREAS
AIR SIDE = 0.0193 ft^2
GAS SIDE = 0.0295 ft^2

HEAT - TRANSFER AREAS
AIR SIDE (A_a) = 2.34 ft^2
GAS SIDE (A_g) = 2.49 ft^2

HYDRAULIC DIAMETERS
AIR SIDE (D_a) = 0.157 ft.
GAS SIDE (D_g) = 0.0892 ft.

fig. 5

PREDICTED THERMAL OUTPUT OF THE STRAIGHT TUBE EXCHANGER

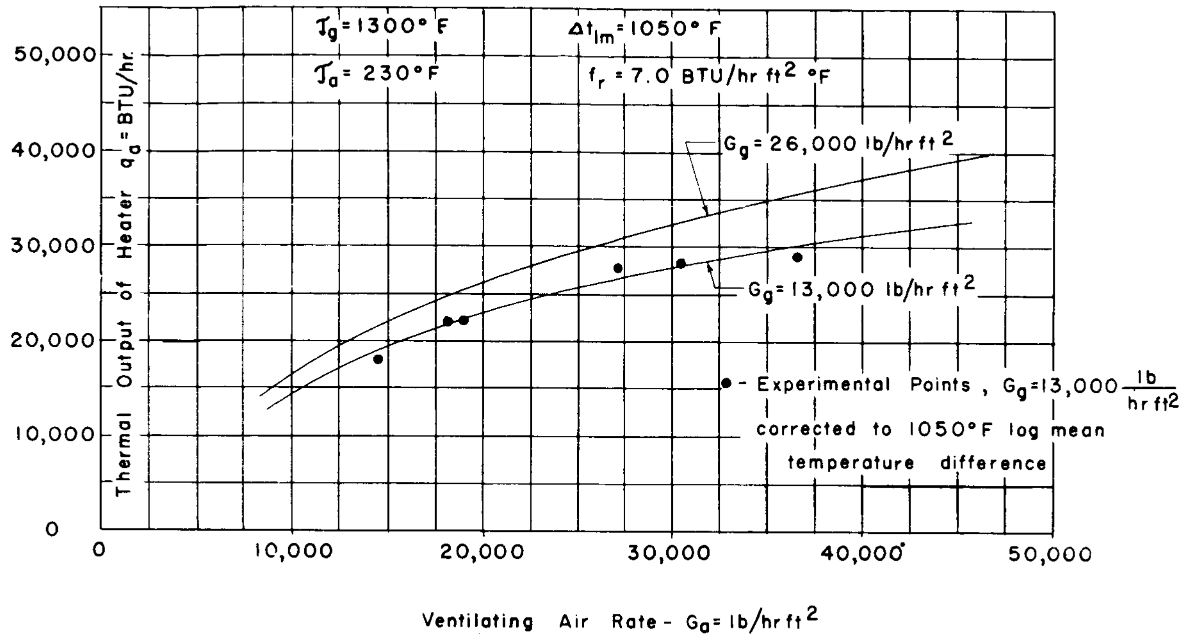

fig. 6

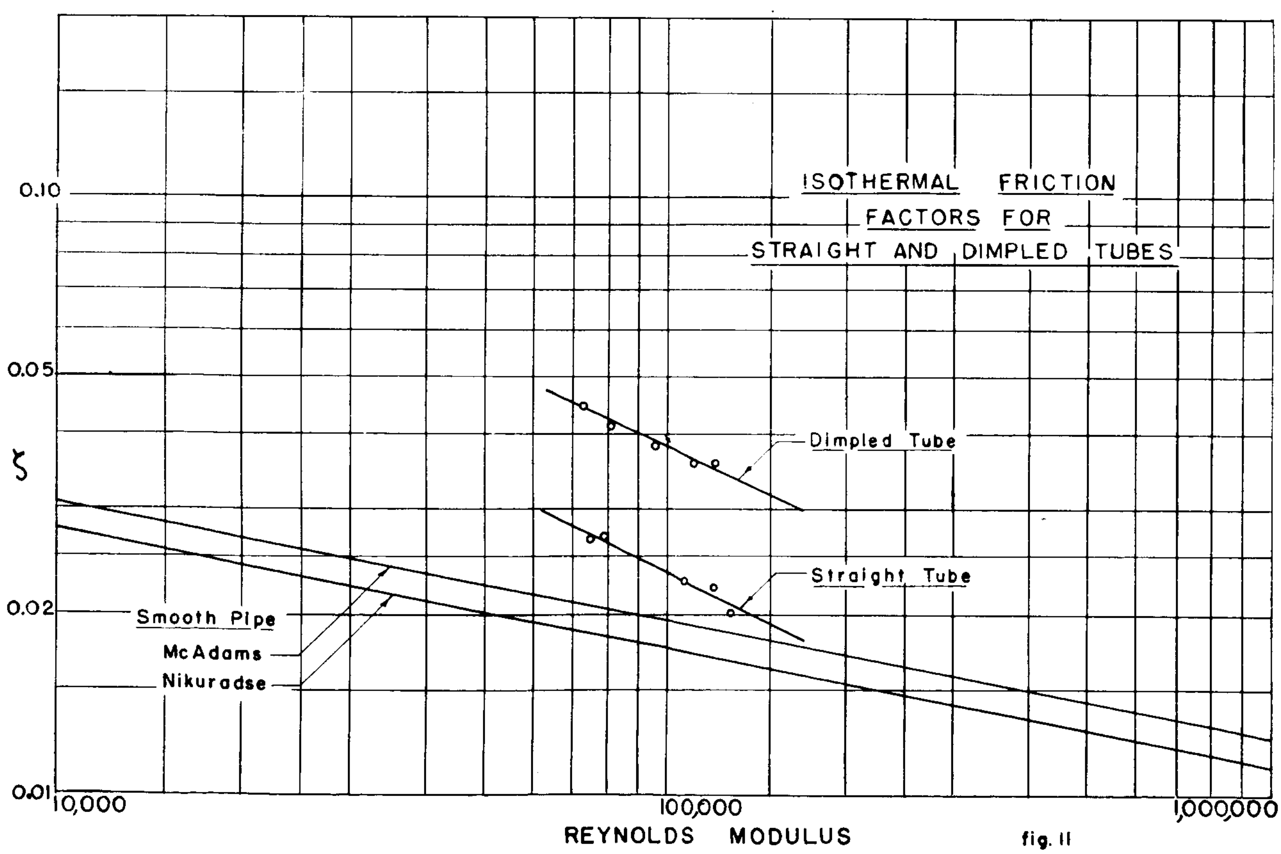

fig. 11

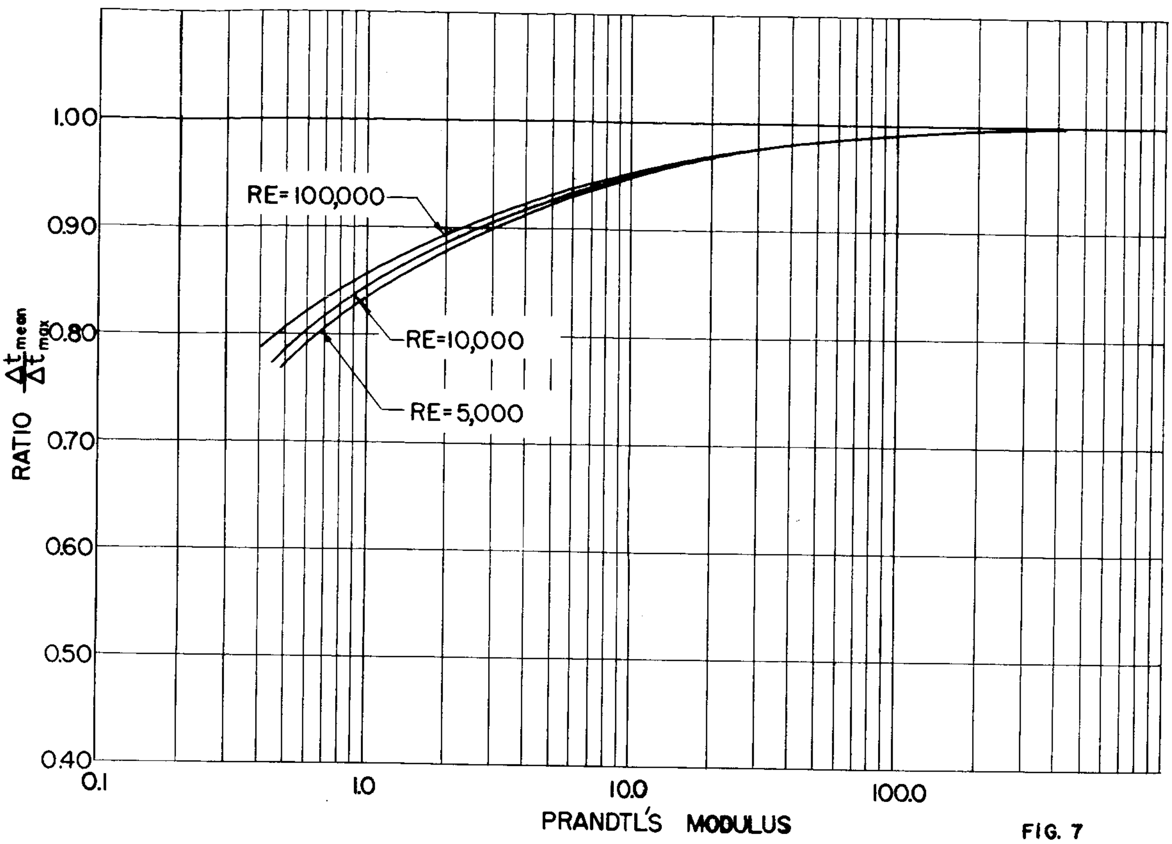

FIG. 7

TEMPERATURE DISTRIBUTIONS AT OUTLET OF STRAIGHT AND DIMPLED TUBES WITHOUT MIXING CHAMBERS

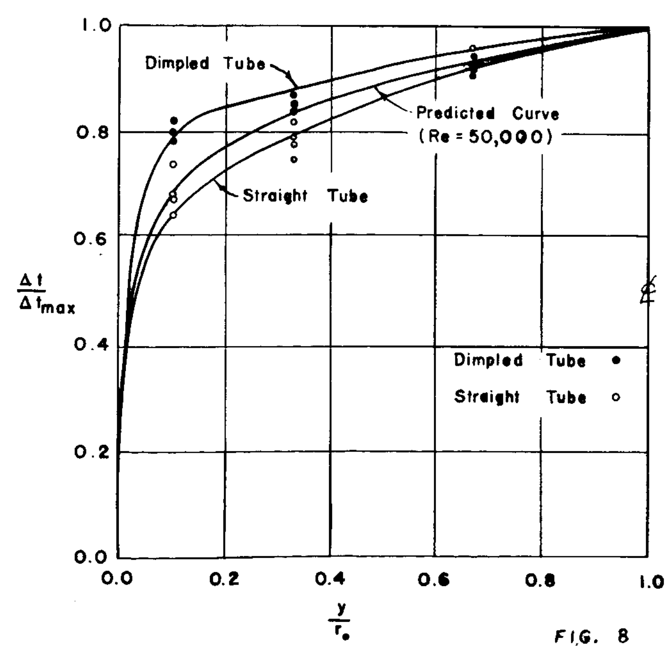

FIG. 8

ISOTHERMAL & NON ISOTHERMAL PRESSURE DROP FOR STRAIGHT TUBE

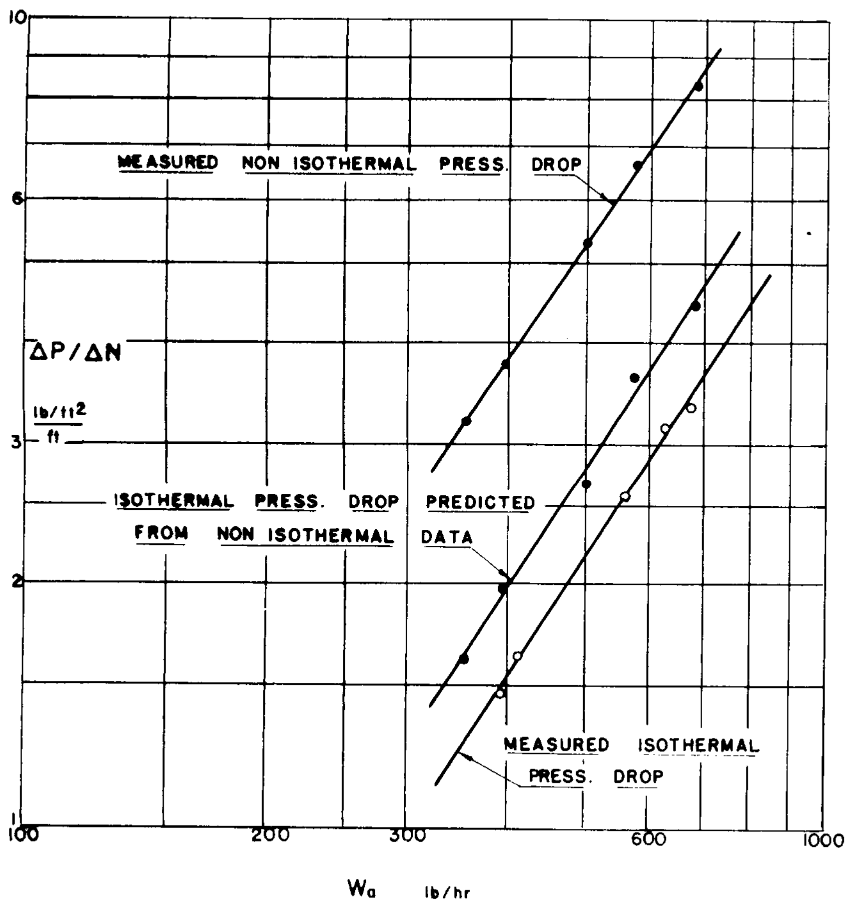

fig. 9

ISOTHERMAL & NON ISOTHERMAL PRESSURE DROP FOR DIMPLED TUBE

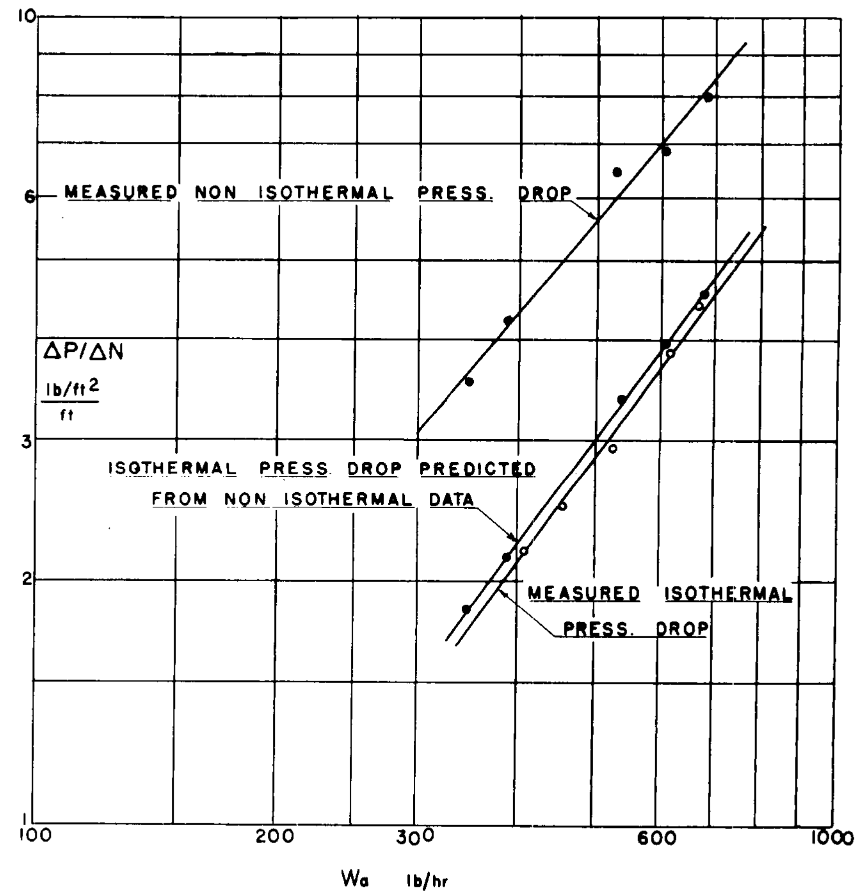

fig. 10

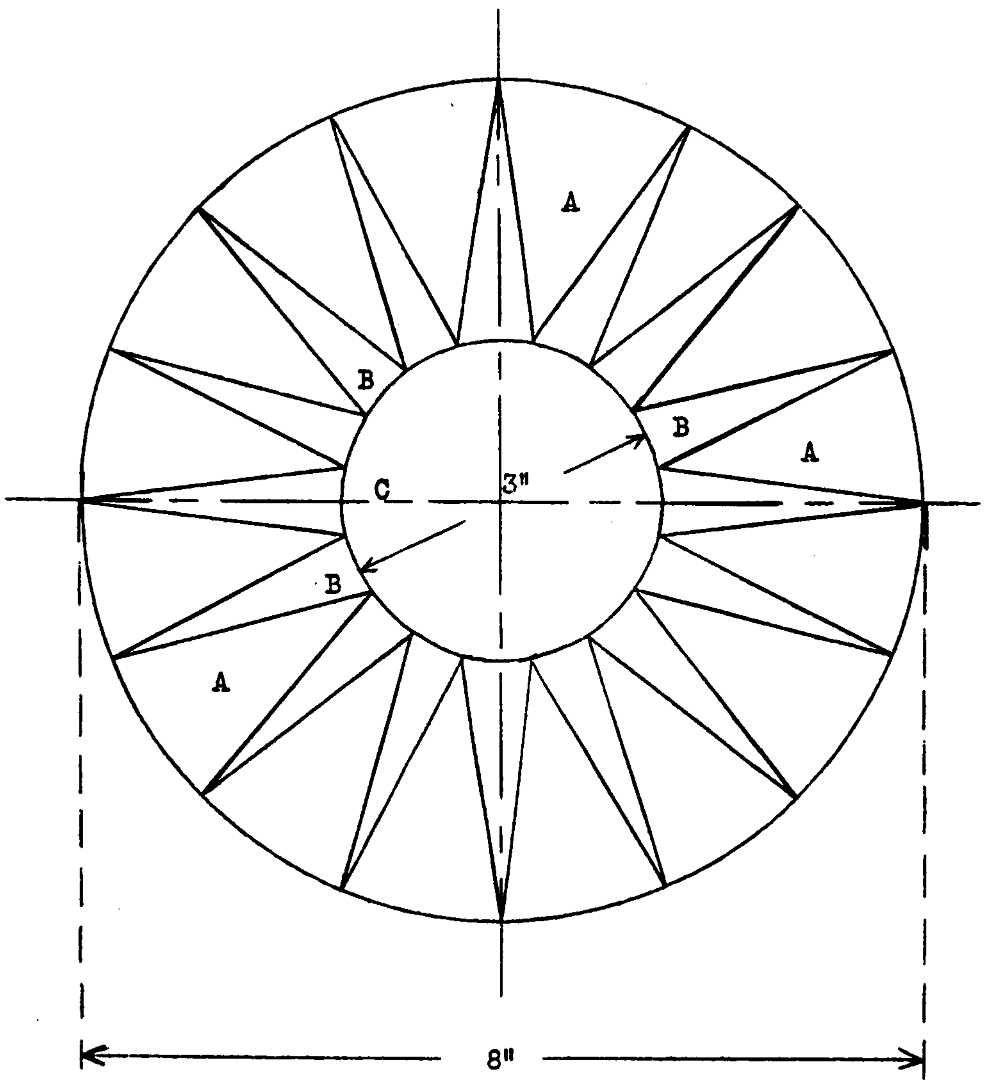

Figure 12.